Modulation of Type IV pili phenotypic plasticity through a novel Chaperone-Usher system in *Synechocystis sp.*

Anchal Chandra[a,1], Lydia-Maria Joubert[b], Devaki Bhaya[a,1]

Author affiliation:
[a] Department of Plant Biology, Carnegie Institution for Science, 260 Panama Street, Stanford, CA940305, USA
[b] *CSIF,* Stanford University Medical Center, Stanford, CA 94305-5301 USA

[1]*Corresponding author:*
Name: Anchal Chandra
Email: anchal.chandra@gmail.com
Address:
Carnegie Institute for Science
260 Panama Street, Stanford, CA-94305

and

Name: Devaki Bhaya
Email: dbhaya@carnegiescience.edu
Address:
Carnegie Institute for Science
260 Panama Street, Stanford, CA-94305

Running title: Modulation of phenotypic plasticity of Type IV pili

Keywords: Phenotypic plasticity/ Type-IV Pili/ Chaperone-Usher */* Phototaxis/ *Synechocystis sp. PCC6803*/ Social motility

Abstract

48
49   Controlling the transition from a multicellular motile state to a sessile biofilm is an important
50   eco-physiological decision for most prokaryotes, including cyanobacteria. Photosynthetic and
51   bio geochemically significant cyanobacterium *Synechocystis sp.* PCC6803 (*Syn6803*) uses Type
52   IV pili (TFP) for surface-associated motility and light-directed phototaxis. We report the
53   identification of a novel Chaperone-Usher (CU) system in *Syn6803* that regulate secretion of
54   minor pilins as a means of stabilizing TFP morphology. These secreted minor-pilins aid in
55   modifying TFP morphology to suit the adhesion state by forming cell to surface contacts when
56   motility is not required. This morphotype is structurally distinct from TFP assembled during
57   motile phase. We further demonstrate by examining mutants lacking either the CU system or the
58   minor-pilins, which produce aberrant TFP, that are morphologically and functionally distinct
59   from wild-type (WT). Thus, here we report that in *Syn6803*, CU system work independent of
60   TFP biogenesis machinery unlike reported for other pathogenic bacterial systems and contributes
61   to provide multifunctional plasticity to TFP. cAMP levels play an important role in controlling
62   this switch. This phenotypic plasticity exhibited by the TFP, in response to cAMP levels would
63   allow cells and cellular communities to adapt to rapidly fluctuating environments by dynamically
64   transitioning between motile and sessile states.

65

66   **Significance of this work**
67   How cyanobacterial communities cope with fluctuating or extreme environments is crucial in
68   understanding their role in global carbon and nitrogen cycles. This work addresses the key
69   question: how do cyanobacteria modulate external appendages, called Type IV pili, to effectively
70   switch between motile and sessile biofilm states? We demonstrate that cells transition between
71   forming strong cell-surface interactions indispensable for biofilm formation to forming cell-cell
72   interactions that allow for coordinated movement crucial for social motility by functional/
73   structural modification of same TFP appendage. The second messenger, cAMP and a Chaperone-
74   Usher secretion are indispensible to achieve these structural modifications of TFP and control the
75   complex phenotypic transition. We have uncovered a strategy that *Syn*6803 has evolved to deal
76   with molecular decision-making under uncertainty, which we call phenotypic plasticity. Here we
77   demonstrate how a single motility appendage can be structurally modified to attain two
78   antagonistic functions in order to meet the fluctuating environmental demands.

79

80   **Introduction**
81   To sustain life in both terrestrial and aquatic environments, cyanobacteria can form multicellular
82   light-driven motile communities or sessile, multi-species biofilms encased in an extracellular
83   polysaccharide (EPS) matrix. In pathogenic bacteria, where the transition from a planktonic
84   motile state to a sessile biofilm has been extensively studied and requires the expression of
85   flagella, which is turned off as the community progresses into a biofilm state. Type IV pili (TFP)
86   and EPS [1] are synthesized at this stage to facilitate surface adhesion instead of motility. There is
87   an ordered progression towards a complex biofilm state[2] and the physiology of bacteria within a
88   biofilm is distinct from the same cells in a planktonic state[1]. TFP in pathogenic bacteria are
89   currently assigned a role only in the surface-associated adhesion required for biofilm related
90   social behavior. Several proteins are required for the biogenesis, assembly and function of TFP[3,]
91   [4] which has been studied in the multicellular swarms of *Myxococcus. xanthus*[5], and in the
92   pathogens *Pseudomonas aeruginosa*[6], *Neisseria gonorrhoeae*, *Escherichia coli* and *Vibrio*
93   *cholerae*[7, 1].

94   In contrast, little is known about the regulation of social behavior of environmentally relevant
95   phototrophs. Notably, many members in the phylum Cyanobacteria encode TFP[8] but none are
96   reported to encode flagella[9]. This suggests that cyanobacteria are likely to use different strategies
97   to switch between motile and sessile states. Here we report that the phenotypic plasticity of the
98   TFP allows *Synechocystis* sp. PCC 6803 (hereafter *Syn6803*) cells to control switching between
99   these states. *Syn6803* cells are capable of 'twitching' or 'gliding motility' over wet surfaces
100 using TFP. *Syn6803* cells also exhibit motile social behavior that can be regulated by the
101 direction, intensity and wavelength of light, a phenomenon known as phototaxis[10]. Mutants
102 lacking structural and regulatory components of TFP exhibit a variety of motility phenotypes[11,]
103 [12]. For instance, *Syn6803* lacking *pilA1* (*sll1694*), which encodes pilin, the major structural
104 component of TFP, are non-motile and lack TFP[13]. Phototaxis in *Syn6803* additionally requires
105 multiple photoreceptors[14, 15, 16, 17] and a complex signaling network[10, 17]. Furthermore, cells that
106 cannot synthesize adenylyl cyclase (Δ*cya1*) exhibit limited motility[18, 19]. In this work we
107 demonstrate that the Δcya1 strain makes structurally aberrant TFP that might explain their
108 limited motility and that addition of extracellular cAMP rescues TFP function and morphology,
109 as well as motility.
110
111 In some bacteria, a dedicated secretion system comprised of a chaperone and usher (CU) protein
112 is upregulated during biofilm formation. This system is required for the transport and assembly
113 of secondary structures (fimbriae, curli[20]) at the cell surface that promote cell-adhesion. The CU
114 pathway serves as a minimal secretion system that allows for protein secretion without energy
115 (ATP) consumption[21, 22, 23]. We have identified a CU system in *Syn6803* that appears to play a
116 novel role in assisting the modification of TFP rather than in the secretion of secondary adhesive
117 appendages.
118
119 To identify the role of this novel CU system and function of its secreted products, we took
120 several complementary approaches. We used biochemical and pull-down assays to show that the
121 putative CU system was involved in secretion of minor-pilins and an adhesin-like protein to the
122 cell surface which serve complementary, yet distinct roles, in modifying TFP and the cell
123 surface. Finally, we exploited gene-specific mutants to help dissect the complex relationship
124 between TFP function and motility phenotypes by using phototaxis assays and electron
125 microscopy. We also determined that cAMP was involved in the regulation of motility via these
126 secreted products.
127
128 Based on these results, we present a preliminary model to explain how cell communities
129 transition between motile and sessile states. The model also highlights the central role of cAMP
130 in regulating several key components, including a novel CU system and minor-pilins that modify
131 the functional behavior of the TFP. We propose that *Syn*6803 can rapidly alter TFP function,
132 which changes the propensity of pili to adhere to surfaces (or other cells) or to glide over
133 surfaces. This phenotypic plasticity exhibited by the TFP allows cells and communities to deal
134 with molecular decision-making under uncertainty.
135
136   **Results**
137 **cAMP controls TFP assembly**
138 cAMP is a ubiquitous second messenger involved in signal transduction in bacteria and
139 eukaryotes. Adenylyl cyclase converts ATP to 3′, 5′-cyclic AMP (cAMP) which binds catabolite

3

140 receptor protein (CRP). The cAMP-CRP complex in turn, activates or represses transcription of
141 downstream genes by binding to a conserved palindromic motif (TGTGAN$_6$TCACA)[24]. *Syn6803*
142 encodes a CRP (Sycrp1; sll1371) and an adenylyl cyclase (Cya1; slr1991)[19]. When WT cells are
143 spotted on soft agarose plates, motile cells phototax to the front of the drop and then move out
144 making typical long finger-like projections. Δ*cya1* cells are motile but exhibit an aberrant
145 behavior; they aggregate at the front of the drop but rarely move beyond the front (**Fig. 1A,**
146 **upper panel**). This impaired motility phenotype can be rescued in Δ*cya1* cells by the addition of
147 extracellular cAMP (0.1mM) (**Fig. 1A, lower panel**). To investigate the cause of this impaired
148 motility, we first examined the TFP of WT and Δ*cya1* cells by negative staining followed by
149 transmission electron microscopy (TEM) (**Fig. 1B, upper right panel**). WT cells (**Fig. 1B,**
150 **upper left panel**) typically exhibited several long TFP (> 2μm, 0.006± 0.002mm width), which
151 were often connected to neighboring cells. Surprisingly, Δ*cya1* cells had none of these long TFP
152 but only a few (~4-5) very short, tapered (~0.2μm length, 0.03 mm± 0.013 width) surface
153 structures.
154
155 We reasoned that if cAMP was able to rescue the motility behavior of the Δ*cya1* cells we should
156 also be able to observe the short structures transition back to long TFP. First, we verified that
157 cAMP could enter cells when added extracellularly, by using a competitive enzyme
158 immunoassay (**Fig. S1a**). This showed that there was a slow increase in intracellular cAMP
159 levels over time, after addition of cAMP to the agarose plate. When we supplemented cells with
160 extracellular cAMP (0.1mM) for 20 hours (**Fig. 1B, lower panels**), and examined TEM images,
161 we found that cells now exhibited TFP similar to WT cells. This indicated that cAMP actively
162 controls the assembly of long TFP and in its absence short, but functional, TFP are formed. Thus,
163 cAMP might mediate correct TFP assembly either by directly controlling pilin expression levels
164 or by controlling the synthesis of additional proteins that are required for TFP function or
165 stability. To distinguish between these two possibilities, we used qRT-PCR to check if *pilA1*
166 (encoding the major TFP pilin) and other previously identified pilin-like proteins (*pilA2-A8*)
167 were controlled by cAMP. There was no change in *pilA1* levels or other pilin assembly genes in
168 Δ*cya1* cells, supplemented with cAMP (**Fig. S1b**), indicating that cAMP does not directly
169 regulate pilin (PilA1) synthesis. Alternatively, cAMP could regulate TFP assembly by
170 controlling the activity of other genes. To identify these putative genes, we used two approaches.
171 First, we identified genes and operons that contained predicted upstream conserved CRP binding
172 sites[23]. Second, we focused on genes that had been reported to be strongly down-regulated in
173 Δ*Cya1* cells[25][26]. Two putative operons met these criteria, the first contained two genes (slr1667,
174 slr1668) and the other contained four genes (slr2015, slr2016, slr2017 and slr2018). Using qRT-
175 PCR, we showed that addition of extracellular cAMP restored the expression levels of all of
176 these genes, close to WT levels in Δ*Cya1* cells (**Fig. 1C**). This suggested that some or all six of
177 these gene products might affect TFP-dependent motility and so we used complementary
178 approaches to identify their specific roles.
179
180 **Identification of a novel Chaperone-Usher (CU) system in *Syn6803* that is regulated by**
181 **cAMP**
182 The genes slr1667 and slr1668 comprise an operon with a canonical cAMP receptor (SyCRP1)
183 binding site (**TGTGA**TCTGGG**TCACA**) upstream (**Fig. 2A**). slr1668 is highly homologous to
184 the chaperone protein of the CU system[21, 27, 28] and shows 87% overall conservation and greater
185 than 67% conservation in the structural motifs and residues characteristic of the FGS sub-family

4

186 members (chaperone proteins that contain a **s**horter loop between **F**1 and **G**1 beta strands) (**Fig.**
187 **S2a**) that is vital for chaperone function. An overlay of the crystal structure of the evolutionarily
188 related PapD, FimC chaperones with a homology model of slr1668 revealed two
189 immunoglobulin-like domains characteristic of the chaperone family proteins (**Fig. S2b**). slr1667
190 encodes a protein of 178aa with very low homology to a fimbrial protein (**Fig. S2d**), although the
191 N-terminal contains a 25aa signal peptide and a typical Sec-like secretion signature motif. Using
192 a Hidden Markov model (HMM) we identified divergent repeat units (24-40aa and 47-64aa)
193 (**Fig. S2c**). Such repeats are characteristic of fimbrial tip adhesins secreted via the CU pathway
194 and suggest that slr1667 may be secreted via the CU system. Previously, it was shown by
195 immunocytochemical analysis that slr1667 is localized at the cell surface, while slr1668 is
196 localized in the cell periplasm[29]. Therefore, we refer to slr1668 as '*chpA'* (chaperone) and
197 slr1667 as '*adhA'* (adhesin).
198
199 Typically, genes encoding CU components are organized in an operon that includes three
200 proteins: the chaperone, the usher and a fimbrial subunit, such as an adhesin [21]. In *Syn6803,* we
201 identified a putative usher homolog, slr0019 which had 30% identity to the usher, FimD (**Fig.**
202 **S2e**) but it is not adjacent to '*adhA'* and '*chpA'*. However, in other sequenced cyanobacterial
203 genomes, the three proteins, chaperone, usher and adhesin are in predicted operons (**Fig. S2f**).
204 We thus refer slr0019 as the usher or '*ushA'*. Notably, all the cyanobacterial genomes encoding a
205 CU system also contained homologues of pilin biosynthesis genes (**Fig. S2g**) suggesting that
206 they may have inter-related functions. Thus, *Syn*6803 have a putative CU system consisting
207 minimally of ChpA, AdhA and UshA. Next we investigated the role of this putative CU system
208 in motility.
209
210 **The Chaperone-Usher system secretes AdhA and minor-pilins (slr2015-slr2018)**
211 To investigate if the chaperone, ChpA, was involved in transport of the putative adhesin, AdhA,
212 we performed *in-vitro* pulldown assays using His tagged-AdhA and GST-ChpA. ChpA forms a
213 stable complex with AdhA (**Fig. 2B**) suggesting that AdhA is transported out of the cell by the
214 CU system, which is also consistent with its localization to the cell-surface[29]. Next, to establish if
215 proteins other than AdhA were transported by the CU pathway, we performed *in-vivo* pulldowns
216 (**Fig. 2C**). *Syn6803* whole cell lysate was incubated with GST-ChpA immobilized on GST
217 magnetic beads, as bait. Several proteins were pulled down by GST-ChpA. Protein bands that
218 were clearly visible with Sypro-Ruby stain were excised from SDS-PAGE and processed for
219 analysis by mass mapping (MALDI-MS/MS). This clearly identified slr2018 as an interacting
220 partner of ChpA (**Fig. 2C**). Low levels of other proteins could be seen in the ChpA pulldown
221 assay but were hard to identify with MALDI-MS/MS (based on their size, these may have
222 included previously identified slr2015, slr2017). The slr2018 polypeptide (~96kDa) is encoded
223 by the last gene in a putative operon that includes slr2015, slr2016 and slr2017. As described
224 earlier, slr2018 is in a putative operon which is likely to be controlled by cAMP based on genetic
225 and bioinformatics.
226
227 The N-terminal hydrophobic regions of slr2015, slr2016, slr2017 exhibit significant conservation
228 to Type IV prepilins from Gram-negative pathogens and cyanobacteria (**Fig. S2h**) with a
229 conserved peptidase cleavage site ($G_{F/V/Y}X\underline{L}XE$) recognized by the PilD signal peptidase[3].
230 slr2018 gene product has a somewhat unconventional N-terminal region (G_FXXXE). These gene
231 products were previously identified as PilA9 (slr2015), PilA10 (slr2016), PilA11 (slr2017)[11] and

5

232 we extended the same nomenclature to include slr2018 as 'PilA12'. Based on this preliminary
233 identification, we refer to these as 'minor-pilins'. Minor-pilins have been identified for other
234 pathogenic bacterial systems and play an essential role in priming TFP assembly in *P.*
235 *aeruginosa* [30].
236
237 **Mutants in the CU system and minor-pilins display different motility phenotypes**
238 To further probe the interactions between the CU system and the minor pilins we examined the
239 motility behavior of the *ΔushA, ΔchpA* and*Δ adhA* mutants. We also took advantage of existing
240 gene-specific, nonpolar mutants of minor-pilins, *pilA9, pilA11* and *pilA12*[13, 26] to further identify
241 the exact role of minor-pilins in *Syn6803* in TFP mediated motility.
242
243 *ΔushA cells exhibit hyper-motile behavior*
244 We reasoned that if the CU pathway and its partner proteins were critical for motility, mutants in
245 this pathway should exhibit motility defects. We characterized the motility phenotypes of *ΔchpA*,
246 *ΔadhA* and *ΔushA* mutants and the minor-pilin mutants, slr2015 (*pilA9*), slr2017 (*pilA11*) and
247 slr2018 (*pilA12*) that were generated either by double homologous recombination or by
248 transposon mutagenesis (**Table** S**1**, S**2**). *ΔushA* cells exhibited two unique motility behaviors
249 (**Fig. 3A**). As expected, WT cells phototaxed to the front of the drop and then after ~24-30h,
250 emerged as finger-like projections of motile cells. Surprisingly, *ΔushA* cells, developed finger-
251 like projections much faster than the WT cells, as early as 15h (**Fig. 3A, left panel, Fig. S3a**).
252 This was consistent with the quantification of the mean velocity and speed of the WT and *ΔushA*
253 cells, over time. For instance, at 12h, the velocity of *ΔushA* cells was thrice that of WT cells
254 (**Fig. 3B, 3C, Fig. S3b, Table S3**). Second, we routinely observed that although the majority of
255 motile WT cells phototaxed to the drop front, many small groups of cells remained "stuck" on
256 the agarose. However, the *ΔushA* mutants did not appear to "stick" to the surface (**Fig. 3A, right**
257 **panel**). This suggested that there might be cell-surface protein(s) that makes the cell "sticky" in
258 WT cells, which are absent from the cell surface of *ΔushA* cells. Consequently, cells do not
259 adhere to other cells or to the agarose surface, resulting in a 'hyper-motile' phenotype.
260
261 *Minor-pilin mutants are non-motile*
262 In contrast to the hyper-motile *ΔushA* cells, the three minor-pilin mutants (*ΔpilA9, ΔpilA11,*
263 *ΔpilA12*) were completely non-motile (**Fig. S3c**), based both on the phototaxis assay and by
264 measurements of cell movement that indicated that there was no displacement over time. These
265 striking differences in the motility behavior of the mutants, ranging from hyper-motile *ushA* cells
266 to non-motile minor pilin mutants, are apparently contradictory, particularly if they are in the
267 same pathway. To reconcile the different phenotypes exhibited by the mutants, we examined
268 other aspects such as (i) TFP biosynthesis, (ii) the morphology and assembly of the TFP and (iii)
269 the ability of TFP to make cell-cell contacts.
270
271 **TFP synthesis, morphology and activity in CU and minor-pilin mutants**
272 (i) *TFP synthesis is not affected in the CU and minor-pilin mutants*
273 To investigate whether the TFP biogenesis machinery or function depends on the CU pathway
274 and/or on the minor-pilins, we analyzed the expression levels of several *pil* genes in the *ΔushA*
275 and minor-pilin mutants (*ΔpilA9, ΔpilA11* and *ΔpilA12*) via qRT-PCR. A core set of conserved
276 proteins required for pilus biosynthesis including PilM, PilN, PilO, PilQ (pilus assembly), PilT
277 PilB1(motor proteins), PilA1, PilA2 (pilins) are found in *Syn6803* and their role in pilus

6

278   assembly has also been inferred from mutant phenotypes[3, 11, 12]. We measured mRNA levels of
279   the following gene homologues: slr1277 (*pilQ*), slr1274 (*pilM*), slr1275 (*pilN*), slr1276 (*pilO*),
280   slr0063 (*pilB1*), sll1694 (*pilA1*), sll1695 (*pilA2*), in the WT and in the mutants. We found that
281   mRNA levels of pilins and components of pilus biogenesis in the mutants were comparable to
282   WT levels (**Fig. S1b, c**). Thus, pilus biosynthesis appears to be unaffected in the CU and minor-
283   pilin mutants and cannot explain the various motility phenotypes.

284

285   *(ii) TFP morphology and assembly is strongly affected in the ΔushA and minor pilin mutant*
286   *strains*
287   Next, we used high resolution TEM to investigate if the distinct motility defects in the mutants
288   could be correlated with changes in TFP morphology (**Fig. 4A**). WT cells have several long TFP
289   (Avg. number 15-20/cell, Avg. length = 2.5μm ± 0.05, Avg. width = 0.007μm± 0.002). The
290   hypermotile ΔushA cells completely lacked long TFP but short stubby structures (Avg. length=
291   0.7mm ± 0.2; Avg. width = 0.02 mm± 0.005) with tapered ends were consistently observed.
292   These TFP were morphologically similar to those previously observed in Δcya1 cells (**Fig. 1B**).
293   On average, there were 5-8 evenly distributed short stubby structures per cell, which are
294   apparently functional, since ΔushA is hyper-motile. Interestingly, the non-motile minor-pilin
295   mutants also exhibited these short, stubby TFP (Avg. length= 0.78mm± 0.21 and 0.63mm ± 0.2).
296   (**Fig. 4B, lower bar graphs**) shows the distribution of TFP and cell sizes (**Fig. S4a**). This clearly
297   indicated that some of the differences in TFP function and motility might be due to different TFP
298   morpho-types (long TFP versus short, stubby TFP). This in turn, might affect their ability to
299   form TFP-dependent intercellular cell-cell contacts.

300

301   *(iii) Mutants exhibit an alteration in the ability to form cell-cell contacts via TFP in the mutants*
302   We then used field emission scanning electron micrography (FE-SEM) to examine TFP
303   morphology and cell-cell surfaces, which revealed another facet of TFP functionality. In WT and
304   ΔushA strains, TFP appear to form strong "cell to cell contacts" which originated around the cell
305   body (**Fig. 4B**). In the minor-pilin mutants, the short TFP appeared to be mostly present at the
306   base of the cell and were involved in forming strong contact with the grid surface rather than
307   cell-surface. The cells were associated in large clusters (**Fig. 4B**) and had a much smoother cell
308   surface than WT (**Fig. S4b**).
309   Consistent with this observation, the crystal violet absorbance assay, a semi-quantitative way to
310   assess cell adherence or biofilm formation, showed that the minor-pilin mutants all had
311   significant adhesion to glass culture vessels, relative to WT cells. In contrast, the usher (ΔushA),
312   chaperone (ΔchpA) and ΔadhA showed greatly reduced (10-30 fold) adherence (**Fig. S4c**). This
313   suggests that secretion of AdhA via CU system is crucial for adhesion of cells. Conversely, in the
314   absence of AdhA, cells experience no counter-force against directed motility and hence are
315   hyper-motile (ΔushA).

316

317   **Discussion**
318   **A new role for a chaperone usher system in TFP assembly**
319   We uncovered a novel role of CU (Chaperone-Usher) system in *Syn6803* which modifies TFP
320   function rather than being involved in secondary filament synthesis as described for most
321   pathogenic bacteria. The *Syn6803* CU system secretes minor-pilins that alter TFP morphology
322   and hence their functionality. In the absence of the usher protein, short TFP are produced but the
323   cells are as motile as WT cells suggesting that long TFP are not strictly necessary for surface

7

324 motility. In support of this, it has been shown that *P.aeruginosa* mutants with very short pili (that
325 are incapable of being sheared) are motile[31]. The CU system also transports AdhA, a cell
326 adhesion/cell surface protein that serves as a crucial component in controlling reversibility of
327 TFP function such that cells can transition between a motile and a sessile state. The ΔushA
328 mutant does not transport the putative adhesin (AdhA), to the cell surface. This results in cells
329 that do not appear to stick to the surface (Fig. S4c) and are hyper-motile relative to WT cells.
330 Such a CU pathway would allow cells to modify TFP function in an energy-independent
331 pathway as well as the cell surface properties in response to cAMP levels. This could allow
332 cyanobacterial populations to make rapid and reversible decisions in response to unpredictable
333 fluctuating environmental variables such as light and nutrients.
334
335 **Switching between pilus morphotypes allows for motile or sedentary lifestyles**
336 Like other bacteria, *Syn6803* undergoes a transition between a motile and sessile (biofilm) state.
337 We demonstrate that TFP in *Syn6803* upon undergoing modification via minor-pilins represent
338 two different morphotypes- long TFP can form strong 'cell to cell contacts' (Fig. 4B, WT and
339 ΔushA) thus facilitate social motility. Second, are the short TFP (Fig. 4B, ΔpilA11, ΔpilA12;
340 FESEM images) that can form strong cell-surface interactions thus facilitating a stable,
341 irreversible transition from motile to sedentary state. This is corroborated by the fact that all the
342 minor-pilin mutants which have short pili appear to attach much more strongly to glass surfaces
343 than WT cells (Fig. S4c). The presence of long TFP might physically obstruct contact with the
344 surface, which can be achieved more effectively by short pili[32]. An alternative explanation is that
345 frequent extension/retraction of dynamic long TFP; keep the cells in motion hence preventing the
346 cells from achieving efficient surface contact[32, 33]. This scenario is in agreement with the finding
347 that surface attachment properties of longer versus shorter type-I and TFP in *Xylella fastidiosa*
348 are distinct[33].
349
350 **Are motility and adhesion mutually exclusive processes?**
351 Surface motility is a complex trait that involves a dynamic interplay between adhesiveness
352 (irreversible attachment to surface) and TFP-driven directional movement in presence of light.
353 The net displacement of cells is an outcome of these two antagonistic forces; i.e. reversible
354 adhesion versus directed movement [32, 34]. The apparent inconsistency between the motility
355 behavior, TFP morphologies and surface adhesion abilities of the various mutants here provides
356 a logical explanation for the distinct yet collaborative role of minor-pilins and AdhA proteins in
357 mediating two processes- motility and adhesion. Motile WT cells assemble long functional TFP
358 and have sufficient AdhA expression on the cell surface. On the other hand, non-motile minor-
359 pilin mutants express same levels of AdhA on the cell surface as WT thus making them highly
360 adherent. However, they lack the ability to secrete minor-pilins that modify/stabilize assembly
361 of long TFP resulting in the short pilus phenotype. Conversely, the surface of hyper-motile
362 ΔushA cells and Δcya1 mutants lack AdhA and minor-pilins which results in short pili and
363 reduced surface adhesion ability; both these phenotypes allow them to move faster than WT
364 cells. The crystal violet binding assay also corroborated that WT cells and minor pilins have
365 stronger cell-surface adhesiveness compared to the ΔushA cells. This leads to the conclusion that
366 short TFP pili are sufficient for motility (Fig. 3A, B), but the ability to adhere to the surface is
367 controlled by AdhA levels. We propose that AdhA that is secreted via the usher pathway to the
368 cell surface[28] and exhibits similarity to fimbrial tip adhesins is crucial for cells to make this
369 decision during the transition stage.

8

370

371 This scenario is in contrast to what has been proposed in most other bacterial systems, where
372 motility and adhesion are antagonistic states and are inversely coordinated[35, 36, 37, 38], In *Syn6803*,
373 we propose there is a dynamic balance between motility and surface adhesion which is required
374 for optimal movement over wet surfaces. We suggest that because surface-dependent motility
375 (here phototaxis) is a group or social behavior, the dynamics cannot be fully explained simply
376 based on the behavior of individual cells. Motility is enhanced by interacting with neighboring
377 cells, mediated by long retractile TFP that can enhance attachment between cells and this
378 enhances certain social behaviors[35]. The dynamic nature of these cellular interactions as seen in
379 motility movies[17] also support the idea that cells need to be "sticky" and "motile" and is
380 maintained by minor pilins and AdhA levels. Finally, this delicate balance is controlled by
381 cAMP levels. (see Model).

382

383 **A model of phenotypic plasticity in Syn6803**
384 Based on our results, we present a model to explain how *Syn6803* dynamically switches between
385 motile and sessile states. cAMP acts as a master regulator to control expression of minor-pilins
386 (PilA9-PilA12) and the CU system (minimally comprised of an usher (UshA), chaperone (ChpA)
387 and adhesion substance (AdhA). Secretion of minor pilins and AdhA to the outside of cell
388 requires CU pathway (**Fig. 5A-upper**). Minor pilins secreted via the CU system help to stabilize
389 TFP and ensure assembly of long TFP that form effective contacts between neighboring cells
390 that is quite crucial for assisted group motility.
391 Transition from surface-associated motility to forming sessile biofilms involves two crucial steps
392 (**Fig. 5B**). The first step involves cells making initial but potentially reversible contacts with
393 surface. Before this stage, cells are still capable of switching back to the motile phase, based on
394 environmental conditions. AdhA expression on the cell surface governs this decision of
395 reversible attachment of cells. The second step of biofilm progression involves those cells that
396 are committed to forming stationary biofilms and form irreversible cell-surface contacts. In the
397 absence or low concentrations of cAMP (**Fig. 5A-lower**), minor-pilins and AdhA are either or
398 absent or expressed at low levels for cells to form short stubby TFP. These functionally modified
399 TFPs are enough to form strong cell to surface contacts to ensure irreversibility and hence
400 commitment to biofilm formation. Future experiments to test these hypotheses, particularly how
401 cell communities control the transition between the motile lifestyle and sessile biofilms will
402 further substantiate our claims.

403
404
405   **Material and methods**
406 *Growth and culture conditions*. Freshwater *Synechocystis sp*. PCC 6803 (*Syn6803*) strain
407 (Berkeley) was maintained in BG-11 medium supplemented with 5mM TES and 10mM
408 NaHCO3 at 30°C with continuous shaking at 100rpm under aerobic conditions and warm white
409 lights (25-30 µmol photons/ m^{-1} s^{-1}). All experiments were performed with cells in exponential
410 phase (O.D$_{730}$= 0.6-0.8). For cell adhesion assays, cells were cultured on bench top without
411 shaking under similar growth conditions.

412

413 *Transcription analysis by quantitative Real-time RT-PCR (qRT-PCR)*. RNA extraction, cDNA
414 synthesis and qRT-PCR measurements were performed as described here[49].

415

9

416 *Agarose motility assays.* Motility assays under directed unidirectional light were carried out at
417 30°C on 0.4% (w/v) Difco agar in BG-11 in 50mm plastic petri dishes (BD falcon-25369022).
418 One microliter of cells (OD_{730} = 0.6-0.8) was placed in the center of a plate. A white LED was
419 used as the light source. The incident light intensity as measured by LI-COR light meter was set
420 to approximately 25µmol photons/ m−1 s−1. For time-lapse video measurements and single-cell
421 tracking analysis see **SI Materials and methods**, Time-lapse imaging and single particle
422 tracking.
423
424 *Electron microscop*y. Detailed description for electron microscopy sample preparation (see **SI**
425 **Materials and methods**, TEM and SEM sample preparation)
426
427 <center>**Acknowledgements**</center>

433

434 <center>**Materials & Correspondence**</center>

435 Dr. Anchal Chandra (achandra@carnegiescience.edu, anchal.chandra@gmail.com)
436 Prof. Devaki Bhaya (dbhaya@carnegiescience.edu)

References

1. Teschler JK, et al. (2015) Living in the matrix: assembly and control of Vibrio cholerae biofilms. *Nat Rev Micro* 13(5):255–268.

2. Guttenplan SB, Kearns DB (2013) Regulation of flagellar motility during biofilm formation. FEMS Microbiol Rev 37(6): 849–871.

3. Giltner CL, Nguyen Y, Burrows LL (2012) Type IV Pilin Proteins: Versatile Molecular Modules. Microbiol Mol Biol Rev 76(4):740–772.

4. Berry J-L, Pelicic V (2015) Exceptionally widespread nanomachines composed of type IV pilins: the prokaryotic Swiss Army knives. FEMS Microbiol Rev 39(1):1–21.

5. Mauriello EMF, Mignot T, Yang Z, Zusman DR (2010) Gliding Motility Revisited: How Do the Myxobacteria Move without Flagella? Microbiol Mol Biol Rev 74(2):229–249.

6. Burrows LL (2012) Pseudomonas aeruginosa Twitching Motility: Type IV Pili in Action. Annual Review of Microbiology 66(1):493–520.

7. López D, Vlamakis H, Kolter R (2010) Biofilms. *Cold Spring Harb Perspect Biol* 2(7). doi:10.1101/cshperspect.a000398.

8. Bianca Brahamsha and Devaki Bhaya (2013) Motility in Unicellular and Filamentous Cyanobacteria. The cell biology of Cyanobacteria, Caister Academic Press, 233-262

9. Schuergers N, Wilde A (2015) Appendages of the Cyanobacterial Cell. *Life* 5(1):700–715.

10. Bhaya D, Bianco NR, Bryant D, Grossman A (2000) Type IV pilus biogenesis and motility in the cyanobacterium Synechocystis sp. PCC6803. *Mol Microbiol* 37(4):941–951.

11. Yoshihara S, et al. (2001) Mutational Analysis of Genes Involved in Pilus Structure, Motility and Transformation Competency in the Unicellular Motile Cyanobacterium Synechocystis sp. PCC6803. *Plant Cell Physiol* 42(1): 63–73.

12. Bhaya D, Watanabe N, Ogawa T, Grossman AR (1999) The role of an alternative sigma factor in motility and pilus formation in the cyanobacterium Synechocystis sp. strain PCC6803. Proc Natl Acad Sci USA 96(6):3188–3193.

13. Bhaya D, Takahashi A, Grossman AR (2001) Light regulation of type IV pilus-dependent motility by chemosensor-like elements in Synechocystis PCC6803. Proc Natl Acad Sci USA 98(13): 7540–7545.

14. Ikeuchi M, Ishizuka T (2008) Cyanobacteriochromes: a new superfamily of tetrapyrrole-binding photoreceptors in cyanobacteria. *Photochem Photobiol Sci* 7(10):1159.

15. Fiedler B, Borner T, Wilde A (2005) Phototaxis in the cyanobacterium Synechocystis sp. PCC 6803: role of different photoreceptors. *Photochem Photobiol* 81(6):1481-8.

16. Song J-Y, et al. (2011) Near-UV cyanobacteriochrome signaling system elicits negative phototaxis in the cyanobacterium Synechocystis sp. PCC 6803. Proc Natl Acad Sci USA 108(26):10780–10785.

17. Ursell T, Chau RMW, Wisen S, Bhaya D, Huang KC (2013) Motility Enhancement through Surface Modification Is Sufficient for Cyanobacterial Community Organization during Phototaxis. PLoS Comput Biol 9(9). doi:10.1371/journal.pcbi.1003205.

18. Agostoni M, Montgomery BL (2014) Survival Strategies in the Aquatic and Terrestrial World: The Impact of Second Messengers on Cyanobacterial Processes. Life (Basel) 4(4):745–769.

19. Bhaya D, Nakasugi K, Fazeli F, Burriesci MS (2006) Phototaxis and Impaired Motility in Adenylyl Cyclase and Cyclase Receptor Protein Mutants of Synechocystis sp. Strain PCC 6803. *J Bacteriol* 188(20):7306–7310

20. Evans, ML., Chapman, MR. (2013). Curli Biogenesis: Order out of Disorder. Biochim Biophys Acta.10.1016/j.bbamcr.2013.09.010.

21. Busch A, Waksman G (2012) Chaperone-usher pathways: diversity and pilus assembly mechanism. Philos Trans R Soc Lond, B, Biol Sci 367(1592):1112–1122.

22. Fronzes R, Remaut H, Waksman G (2008) Architectures and biogenesis of non-flagellar protein appendages in Gram-negative bacteria. EMBO J 27(17):2271–2280.

23. Thanassi DG, Stathopoulos C, Karkal A, Li H (2005) Protein secretion in the absence of ATP: the autotransporter, two-partner secretion and chaperone/usher pathways of gram-negative bacteria (review). Mol Membr Biol 22(1-2):63–72.

11

488   24. Xu M, Su Z (2009) Computational prediction of cAMP receptor protein (CRP) binding sites in
489   cyanobacterial genomes. BMC Genomics 10(1): 23.
490   25. Yoshimura H, Yanagisawa S, Kanehisa M, Ohmori M (2002) Screening for the target gene of
491   cyanobacterial cAMP receptor protein SYCRP1. *Mol Microbiol* 43(4):843–853
492   26. Bhaya D, Takahashi A, Shahi P, Grossman AR (2001) Novel Motility Mutants of Synechocystis
493   Strain PCC 6803 Generated by In Vitro Transposon Mutagenesis. *J Bacteriol* 183(20):6140–6143.
494   27. Geibel S, Waksman G (2014) The molecular dissection of the chaperone-usher pathway. Biochim
495   Biophys Acta 1843(8):1559–1567.
496   28. Costa TRD, et al. (2015) Secretion systems in Gram-negative bacteria: structural and mechanistic
497   insights. Nat Rev Micro 13(6):343–359.
498   29. Yoshimura H, et al. (2010) CccS and CccP are Involved in Construction of Cell Surface Components
499   in the Cyanobacterium Synechocystis sp. strain PCC 6803. *Plant Cell Physiol* 51(7):1163–1172.
500   30. Nguyen, Y. *et al*. Pseudomonas aeruginosa Minor Pilins Prime Type IVa Pilus Assembly and
501   Promote Surface Display of the PilY1 Adhesin. *J Biol Chem* **290,** 601–611 (2015).
502   31. Ackermann M (2015) A functional perspective on phenotypic heterogeneity in microorganisms. Nat
503   Rev Micro 13(8):497–508.
504   32. Jin F, Conrad JC, Gibiansky ML, Wong GCL (2011) Bacteria use type-IV pili to slingshot on
505   surfaces. Proc Natl Acad Sci USA 108(31):12617–12622.Anyan ME, et al. (2014) Type IV pili
506   interactions promote intercellular association and moderate swarming of Pseudomonas aeruginosa.
507   Proc Natl Acad Sci USA 111(50):18013–18018.
508   33. De La Fuente L, et al. (2007) Assessing Adhesion Forces of Type I and Type IV Pili of Xylella
509   fastidiosa Bacteria by Use of a Microfluidic Flow Chamber. Appl Environ Microbiol 73(8):2690–
510   2696.
511   34. Pesavento C, et al. (2008) Inverse regulatory coordination of motility and curli-mediated adhesion in
512   Escherichia coli. Genes Dev 22(17):2434–2446.
513   35. Kaiser D, Crosby C (1983) Cell movement and its coordination in swarms of myxococcus xanthus.
514   Cell Motility 3(3):227–245.
515   36. Fröls, S. et al. UV-inducible cellular aggregation of the hyperthermophilic archaeon Sulfolobus
516   solfataricus is mediated by pili formation. Molecular Microbiology **70,** 938–952 (2008).
517   37. Karatan, E. & Watnick, P. Signals, Regulatory Networks, and Materials That Build and Break
518   Bacterial Biofilms. *Microbiol Mol Biol Rev* **73,** 310–347 (2009).
519   38. Esquivel, R. N., Xu, R. & Pohlschroder, M. Novel Archaeal Adhesion Pilins with a Conserved N
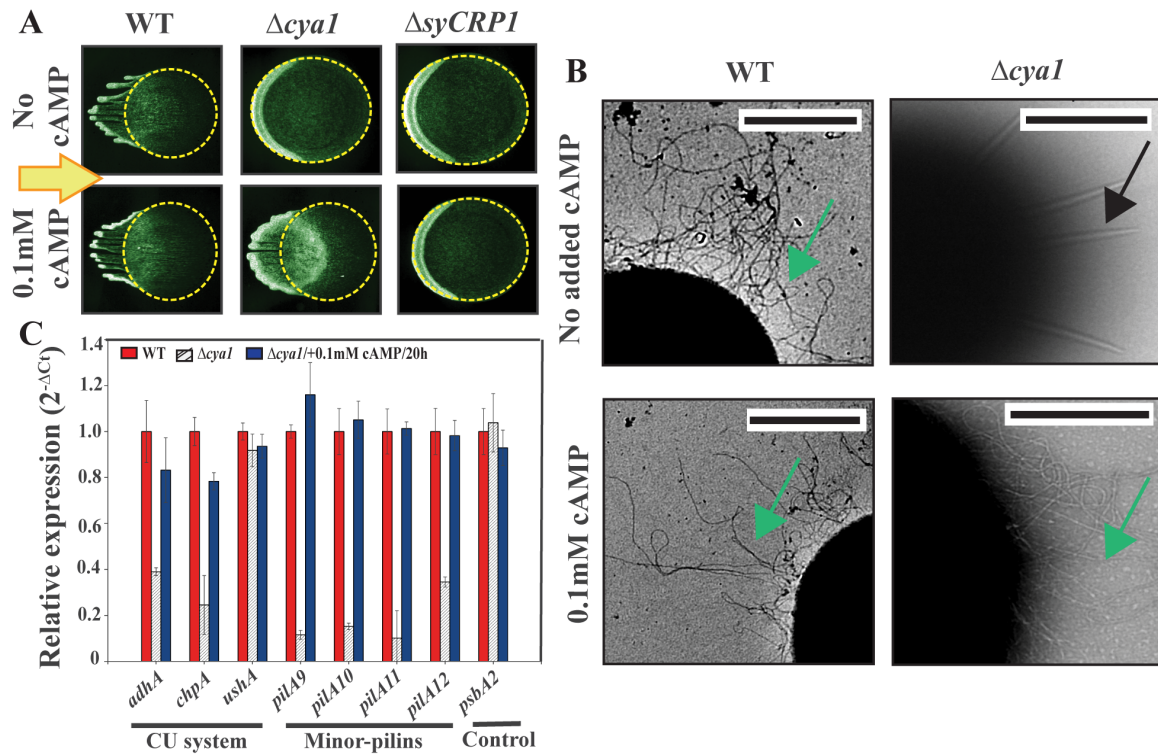520   Terminus. *J Bacteriol* **195,** 3808–3818 (2013).

521
522
523
524
525
526
527
528
529
530
531
532
533
534

Figures

Fig.1: Effect of cAMP on Phototaxis, TFP morphology and transcription in WT and Δ*cya1* and Δ*sycrp1* (complementation assays).

(**A**) *Effect of cAMP on phototaxis*. **Left panel:** WT cells, **Middle panel:** Δ*cya1* cells, **Right panel:** Δ*syCRP1* cells. Motility phenotype after 48h in unidirectional white light 30 μmol m–2 s–1 on the 0.4% agarose plates in the absence (**upper panels**) or presence (**lower panels**) of 0.1mM cAMP. Initial outline of drop (diameter 3-4mm) highlighted in yellow. WT cells make typical finger like projections of groups of moving cells. In the absence of cAMP, both ΔsyCRP1 and ΔCya1 cells accumulate (seen as darker crescent) at front of drop, In the presence of cAMP, Δcya1 cells regain the ability to form finger-like projections similar to WT.

(**B**) *Effect of cAMP on TFP morphology*: Electron micrograph of negatively stained WT (**left**) Δ*cya1* cell (**right**) in the absence (**upper**) or presence 0.1mM cAMP for 20h (**lower**). Stubby, short TFP (black arrow); typical Type IV pili produced in WT and after cAMP addition (green arrow). Scale bar=1μm.

(**C**) *Effect of cAMP on transcript levels*: Bar graph of relative mRNA transcript levels of *chpA, adhA*, and minor-pilin genes in WT cells (red), Δcya1 cells (striped) and Δcya1 cells after incubation with 0.1mM cAMP (blue) quantified by real time PCR (n=3 independent experiments). Error bars denote mean ± s.d where specified. *psbA2* serves as a reference control. C_t values of the reference control were used to normalize the C_{ts} for the gene of interest ($\Delta\Delta C_t$).
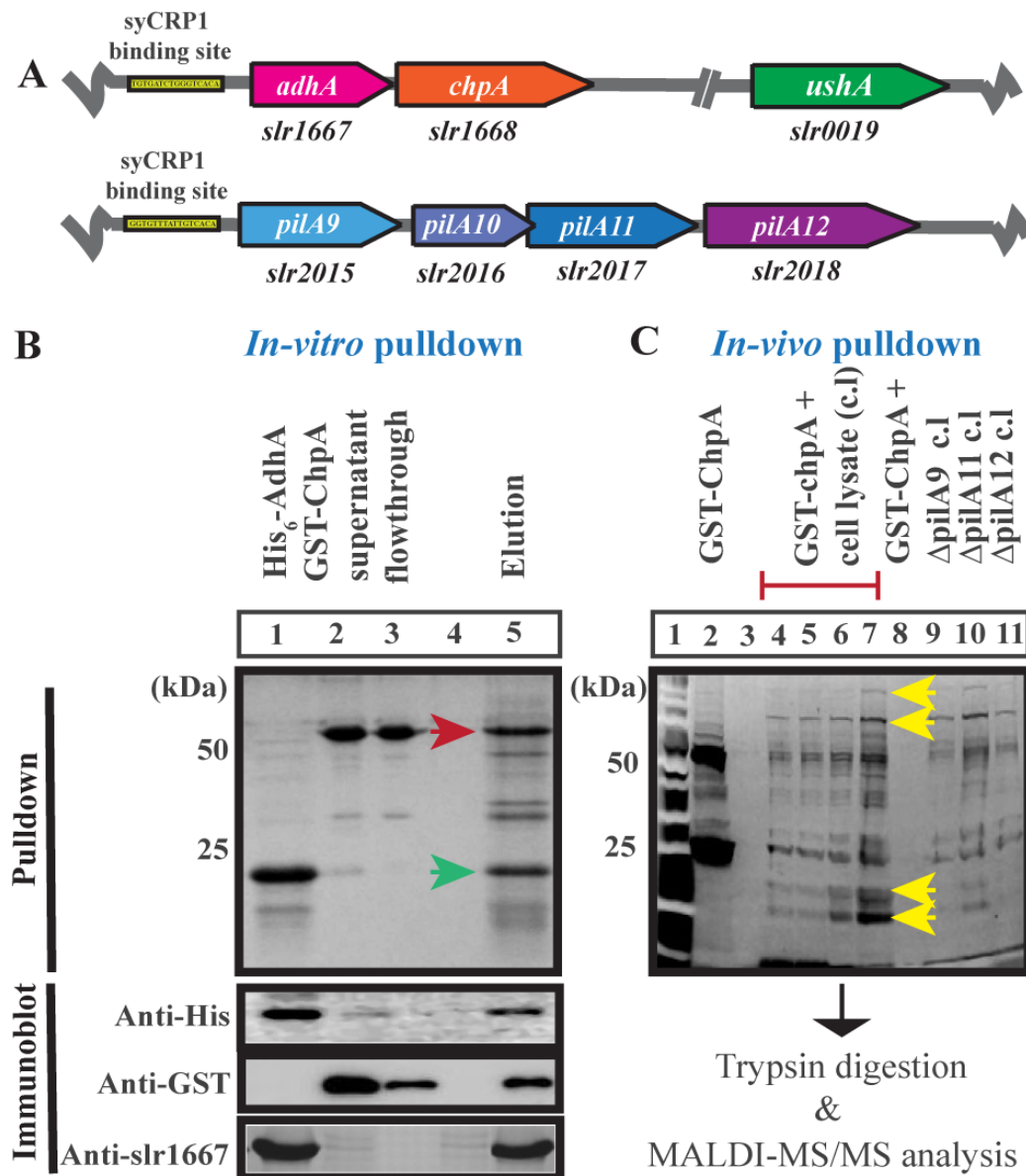
13

Fig. 2: Gene loci regulated by cAMP/Sycrp1 and protein-protein interaction assays.
(**A**) *Organization of gene loci regulated by cAMP* **Top row:** CU system genes **Bottom row:** minor-pilins genes (*pilA9, pilA10, pilA11, pilA12*). SyCRP1 binding site is indicated in yellow box.
(**B**) *In-vitro protein interaction* analyzed by SDS-PAGE. Upper panel: Lane (1) Purified His$_6$-AdhA, (2) GST-ChpA loading, (3) flowthrough, (5) co-eluted His$_6$-AdhA (green arrow~25kDa) and GST-ChpA (red arrow~50kDa). **Lower panel:** Immunoblot with anti-His, anti-GST and anti-AdhA antiserum.
(**C**) *In-vivo GST pulldown assay.* **Upper panel:** Lane (1) protein ladder (2) Glutathione beads with purified GST-ChpA, lane (L4-7) Elution from samples containing beads with GST-ChpA and whole cell lysate of WT *Syn6803* cells. Each of four lanes contains increasing volume of eluted samples. Lanes containing eluted samples of GST-ChpA loaded with whole cell lysates of Δ*pilA9* (L9), Δ*pilA10* (L10), Δ*pilA12* (L11) strains. Yellow arrows indicate samples analyzed using MALDI-MS/MS.
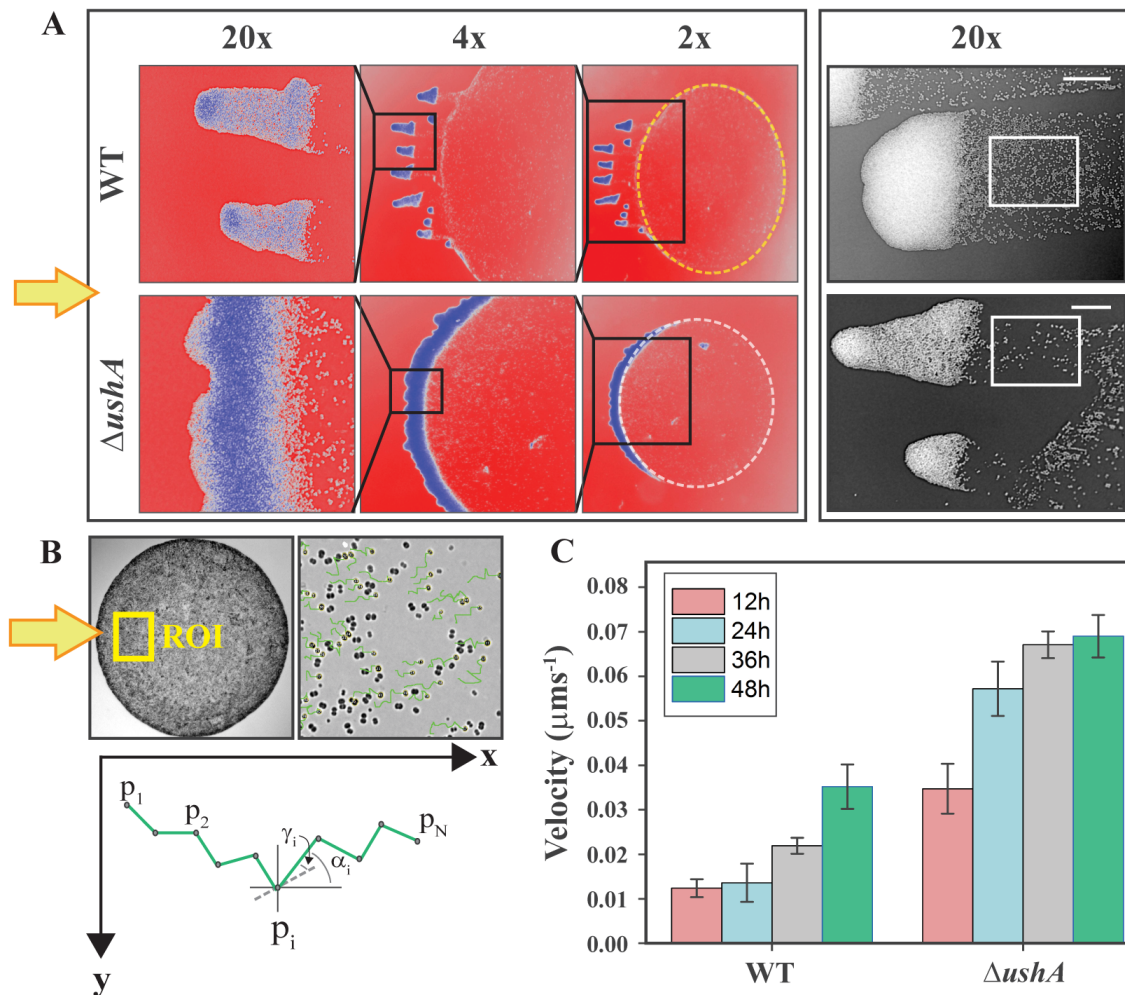
14

572
573
574 **Fig. 3: Hyper-motile ΔushA strain display different motility phenotype under unidirectional light.**
575 (**A**) *Agarose motility assays*: **Left panel:** WT (upper row) and ΔushA (lower row) after 20h motility assay
576 (Arrow indicates direction of light). A small region (black box) from the drop front is magnified at 4x
577 (middle) and 20x (left) to show relative density and movement of cells after first 20h of white light
578 exposure. **Right panel:** 20X magnification of finger front after 48h depicting enhanced collective
579 movement in ΔushA cells (lower) versus WT (upper). See white box. Note how almost no cells are remain
580 in the ΔushA compared to WT. Scale bar~ 20μm.
581 (**B**) **Upper:** Example phase contrast image of the region of the drop used for quantification of average
582 speed and velocity. Scale bar=20μm. **Lower:** The drawing shows a sample trajectory consisting of N
583 points $p_i = (x_i; y_i)$.
584 (**C**) Quantification of mean velocity (in WT versus ΔushA) during different time points (12-48h). Each
585 bar graph represents measurements of 40-50 individual cells for each strain at every time point.
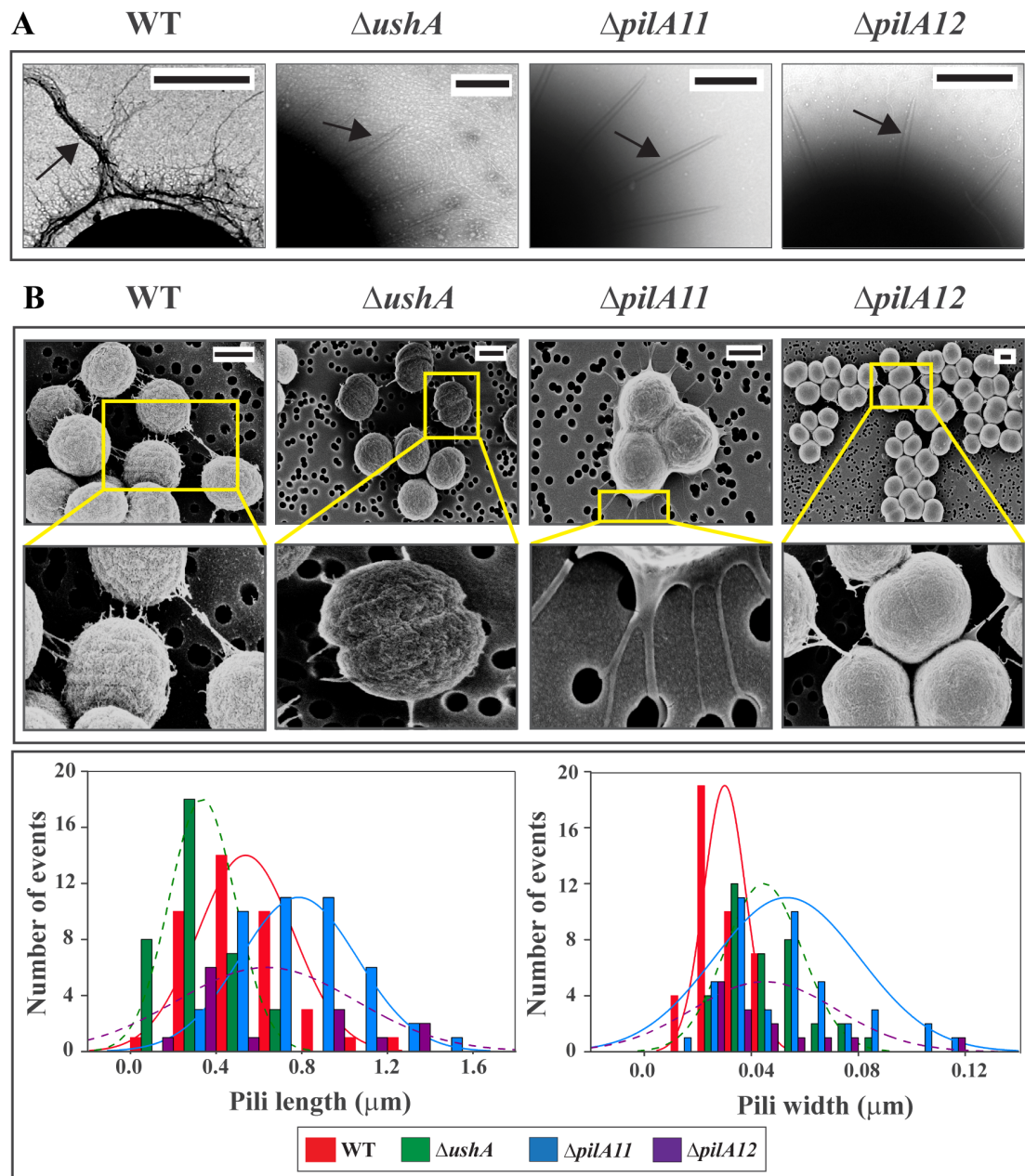586

15

587
588
589 **Fig. 4: Identification of two TFP morphotypes in WT and mutants**.
590 (**A**) *Electron micrographs of negatively stained cells*: WT, Δ*ushA*, Δ*pilA11* and Δ*pilA12* after exposure to
591 unidirectional light on motility plates. Scale 1 μm. Black arrows indicate representative normal TFP.
592 (**B**) *Scanning electron microscopy* **Upper:** SEMs images showing cell-cell interaction (WT, Δ*ushA*) and
593 cell-substrate interaction (Δ*pilA11* and Δ*pilA12*). Respective magnified images (yellow boxes) are shown
594 below to WT and mutants. **Lower:** Left graph: Pilus length distribution in WT and mutant strains, Right
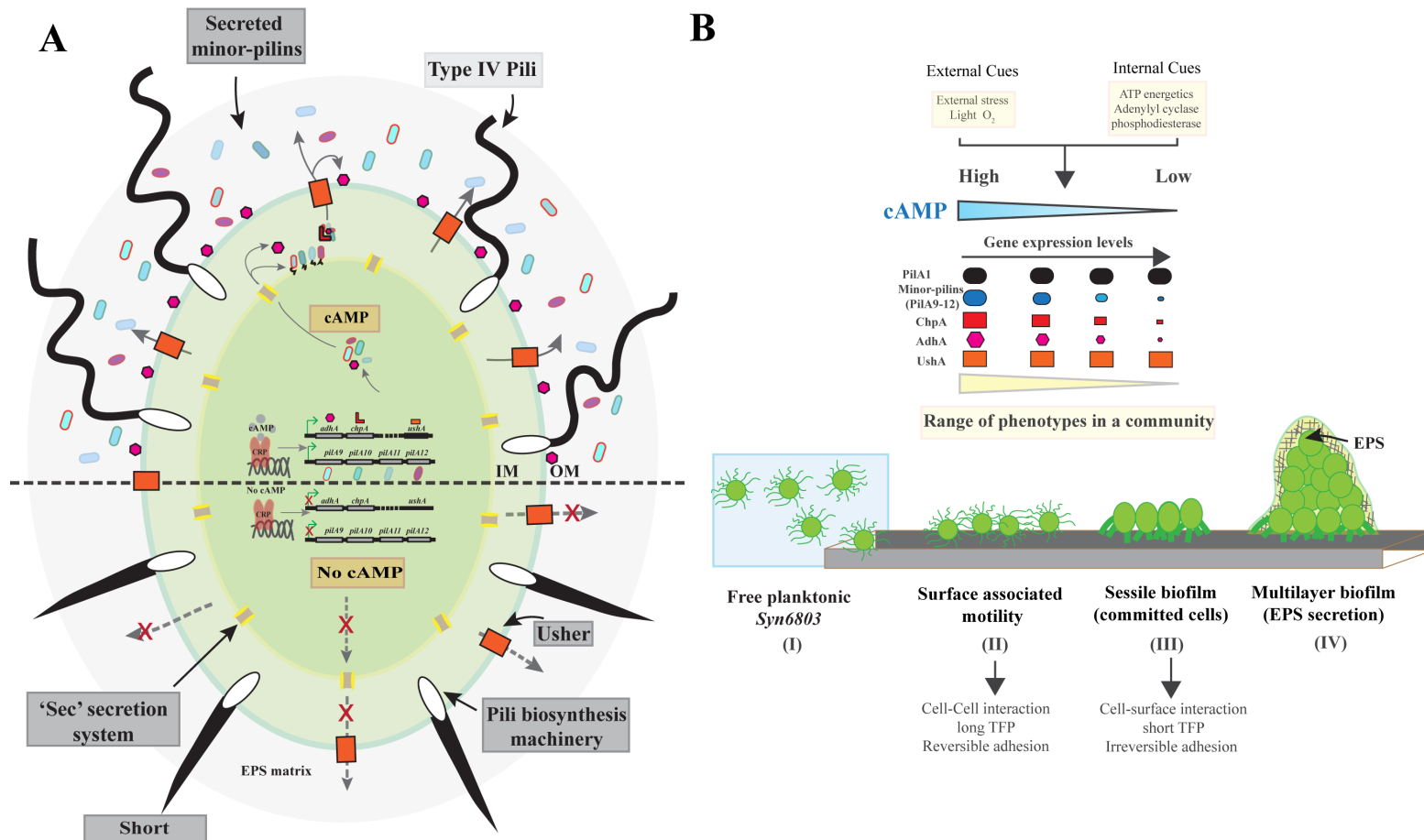595 graph: Pili width distribution.

16

596
597
598
599 **Fig. 5: Model of cAMP regulation of TFP phenotypic plasticity**.
600 (**A**) Individual cell (**B**) Communities showing how dynamic range of effects can be created.